Waste Management 165 (2023) 179–188

Contents lists available at ScienceDirect

Waste Management

journal homepage: www.elsevier.com/locate/wasman

Research Paper

Durability of two bituminous geomembranes (BGMs) with different thicknesses in MSW synthetic leachate

A. Samea [a], F.B. Abdelaal [b,*]

[a] GeoEngineering Centre at Queen's-RMC, Queen's University, Kingston, ON K7L 3N6, Canada
[b] Geotechnical and Geoenvironmental Engineering, GeoEngineering Centre at Queen's-RMC, Queen's University, Ellis Hall, Kingston, ON K7L 3N6, Canada

ARTICLE INFO

Keywords:
Solid waste containment
Bituminous geomembrane
Landfill liner systems
Service life

ABSTRACT

The effect of thickness (4.8 and 4.1 mm) on the degradation of two bituminous geomembranes (BGMs), when immersed in a synthetic leachate is investigated over a period of 33 months. Based on the data collected at four different temperatures (20, 40, 55, 70 °C), it is shown that the 4.1 mm has slightly faster degradation than the 4.8 mm thick BGM. Due to the reduced conditions of the examined leachate, the degradation in the chemical and rheological properties of the bitumen coat was relatively lower than in air and water immersion. However, the presence of a surfactant in the leachate increased the degradation of the polymeric back film and the reinforcement layer responsible for the mechanical properties of the BGM. The time to nominal failure of the two BGMs is predicted at a typical range of landfill liner temperatures using Arrhenius modelling. The predictions at temperatures >20 °C suggest that the examined BGMs may not be suitable for the containment of solid wastes containing surfactants due to the fast degradation in their mechanical properties.

1. Introduction

Geosynthetic barrier systems are widely used in geoenvironmental applications such as landfills, lagoons, and monofills to contain solid wastes, contaminated fluid, or contaminated soils. These mega fills/reservoirs are required by many jurisdictions to be constructed on geosynthetic liners (e.g., MOE, 1998; MPCA, 2005; Alberta Environment Protection Agency, 2010; British Columbia Ministry of Environment, 2016; USEPA, 2016). These liner systems often comprise a geomembrane (GMB) over a low permeability soil layer to function as a composite barrier against contaminant migration into the surrounding environment. Aside from short-term failures due to poor installation or sudden application of external forces, these GMBs are required to have a service life longer than the contaminating life span of the facility which can range from several decades to centuries (Rowe et al., 2000; Rowe et al., 2004). In service, GMBs can be exposed to chemical solutions leaching from solid waste and elevated temperatures that can lead to their degradation and loss of their properties. Under sustained field stresses, this can result in the long-term failure of the GMB liner (Abdelaal et al., 2014a; Ewais et al., 2014) and hence, contaminant migration to the environment. Thus, assessment of the durability of the GMBs and their service lives under field conditions is essential to ensure adequate environmental protection.

Polymeric GMBs, especially high-density polyethylene (HDPE), have been used as a part of the baseliners and cover systems in solid waste containment applications over the last 40 years (e.g., Rowe et al., 2003; Peggs, 2008; Rowe et al., 2010; Gassne, 2017; Li et al., 2021). This led to extensive research that examined their long-term performance and degradation behaviour for these applications (e.g., Schmidt et al., 1984; Maisonneuve et al., 1997; Hsuan and Koerner, 1998; Rowe and Sangam, 2002; Hoor and Rowe, 2012; Abdelaal and Rowe, 2014; Tian et al., 2017; Ewais et al., 2018; Li et al., 2021). Over the last 15 years, bituminous geomembranes (BGMs) have been promoted as a strong candidate liner material for the containment of solid waste due to their high mechanical properties, relatively high density, the possibility of installation in extremely harsh climatic conditions, and low coefficient of thermal expansion (Peggs, 2008; Lazaro and Breul, 2014). They have already been used to line and cap municipal solid waste (MSW) and low-level radioactive waste (LLRW) landfills in jurisdictions and/or applications that do not specify HDPE GMBs for liner or cover systems (Breul et al., 2006; Peggs, 2008; Daly and Breul, 2017; Keys, 2021; Richardson and Wingrove, 2021). However, there is a paucity of research and published data on the durability of BGMs to ensure their proper use in these applications to provide the desired environmental protection.

* Corresponding author.
E-mail addresses: alireza.samea@queensu.ca (A. Samea), fady.abdelaal@queensu.ca (F.B. Abdelaal).

https://doi.org/10.1016/j.wasman.2023.04.031
Received 31 December 2022; Received in revised form 8 March 2023; Accepted 16 April 2023
Available online 12 May 2023

BGMs are multilayer composite materials that are manufactured with thicknesses that range from 3.5 mm to 5.6 mm to provide the desired mechanical and waterproofing properties. BGMs consist of a core nonwoven polyester geotextile (NW-GTX) and a glass fleece sheet as the reinforcement layer that is impregnated and coated with bitumen to create a flexible and impermeable sheet (Peggs, 2008; Bannour et al., 2013). The bitumen used in the production of BGMs is typically stabilized using elastomers such as styrene-butadienestyrene (SBS) (Touze-Foltz and Farcas, 2017) to improve its workable temperature (Scheirs, 2009; Touze-Foltz and Farcas, 2017). The top surface of the BGM is typically sanded to increase the interface friction strength while the bottom surface is bonded to a polyester film to protect the BGM from upward root penetration (Breul et al., 2008; Lazaro and Breul, 2014).

Few studies examined field exhumed BGM samples exposed to UV in different geoenvironmental applications (Addis et al., 2013; Touze-Foltz and Farcas, 2017). These studies showed that the service life of the BGM in the field can substantially vary from several decades (Touze-Foltz and Farcas, 2017) to several months (Addis et al., 2013) depending on the BGM liner temperatures and exposure conditions. For the laboratory studies, Samea and Abdelaal (2023) investigated the durability of BGMs exposed to air and di-ionized (DI) water using immersion tests. It was shown that degradation of the BGMs involves the loss of the viscoelastic properties of the bitumen coat and the loss of the mechanical properties due to the degradation in the reinforcement layer. Based on these results, nominal failure of the BGM as a liner material (i.e., loss of the material resistance) was defined as the time taken for the bitumen coat to reach brittleness or for the BGM to reach 50% of its initial or specified mechanical properties. This study also showed that BGMs can exhibit different degradation rates in their different components when incubated in aqueous solutions. Since the chemistry of the leachates from waste containment application is significantly different and more aggressive than DI water, the chemical compatibility of the BGMs with solid waste leachates is unknown.

In addition to the effect of the chemical composition of the solution in the field on the durability of GMBs, the properties of the GMB have an important role in their long-term performance in the field. Among these properties, the increase in the thickness was shown to increase the durability of polymeric GMBs due to the increase of the diffusion path of the chemicals into the GMB (e.g., Rowe et al., 2010; Rowe et al., 2014; Rowe and Ewais, 2014; Morsy et al., 2021). However, the effect of thickness on the long-term performance of BGMs is also unknown. Thus, the objective of this study is to investigate the long-term performance of two BGMs with different thicknesses when immersed in a synthetic landfill leachate to explore: (a) the effect of BGM thickness on its durability, and (b) the chemical compatibility of BGMs with solid waste leachates.

2. Method and materials

2.1. Materials examined

Two different commercially available BGMs (Table 1) produced by the same BGM manufacturer (denoted as BGM1 and BGM2) were examined in this study. BGM1 is 4.8 mm thick with a mass per unit area of 5200 g/m^2 and is typically recommended for high stress applications. BGM2 is recommended for moderate to low stress applications with a nominal thickness of 4.1 mm and a mass per unit area of 4700 g/m^2. BGM1 and BGM2 have polyester NW-GTXs as the primary reinforcement layer with mass per unit area of 275 and 235 g/m^2, respectively. Additionally, both BGMs have a glass fleece sheet with a mass per unit area of 50 g/m^2. Due to the higher mass per unit area of the NW-GTX and thicker bitumen coat, BGM1 has higher initial puncture resistance, tensile strength, and tensile elongation. The NW-GTX used in manufacturing BGM1 was also examined (Table 1) to compare the degradation of the geotextile to the overall degradation of BGM1.

Table 1
Initial properties of the materials examined (mean ± standard deviation).

Property[a]	Method	BGM1[b]	BGM2[b]	NW-GTX
Designator	–	TERANAP 531 TP 4M	TERANAP 431 TP 4M	–
Nominal Thickness (mm)	ASTM D5199	4.8 ± 0.120 (4.6)	4.1 ± 0.163 (3.9)	1.1 ± 0.128
Glass Mat. Reinforcement (g/m^2)	–	50[c]	50[c]	–
Mass Per Unit Area of the Nonwoven Geotextile Reinforcement (g/m^2)	ASTM D5261	275[c]	235[c]	275
Mass Per Unit Area (g/m^2)	ASTM D5261	5410[c]	4700[c]	263 ± 4.36
Machine Direction Maximum Tensile Strength σ_M (kN/m)	ASTM D7275	33.1 ± 0.422 (25.5)	29 ± 0.852 (24)	–
	ASTM D5035	–		13.4 ± 1.33
Machine Direction Elongation at σ_M (mm)	ASTM D7275	51 ± 1.8 (33)	44 ± 0.16 (28.2)	–
	ASTM D5035	–	–	48 ± 3.7
Cross Machine Maximum Tensile Strength σ_M (kN/m)	ASTM D7275	29.5 ± 0.887 (23)	21.8 ± 0.270 (18)	–
	ASTM D5035	–	–	10.5 ± 0.866
Cross Machine Elongation at σ_M (mm)	ASTM D7275	52 ± 1.5 (35.7)	47 ± 2.1 (30.6)	–
	ASTM D5035	–	–	55 ± 1.2
Puncture Resistance (N)	ASTM D4833	690 ± 41.91 (555)	564 ± 21.91 (467)	627 ± 62.37
Puncture (Break) Elongation (mm)	ASTM D4833	14.35 ± 0.933	12.35 ± 0.61	16.79 ± 0.665
Glass Transition Temperature (°C)	ASTM E2602	−24.2 ± 1.48	−26.10 ± 1.70	82.86 ± 2.27
Complex Shear Modulus (kPa)	–	112 ± 7.38	134 ± 8.80	–
Phase Angle (°)	–	43 ± 0.53	41 ± 0.35	–
Carbonyl Index	–	2.38e-3 ± 5.23e-4	1.99e-3 ± 1.63e-4	–
SBS Index	–	0.014 ± 7.89e-4	0.013 ± 4.62e-4	–

[a] 10 replicates were examined for each property.
[b] Values in parentheses show the minimum specified value by the manufacturer for this BGM.
[c] Values from the manufacturer datasheet.

2.2. Accelerated ageing and incubation fluid

The long-term performance of the BGMs and the NW-GTX was investigated using the immersion technique. This method is used to accelerate the ageing of different geosynthetic materials in the laboratory by immersing coupons into the desired solution at different elevated temperatures (e.g., Hsuan and Koerner, 1998; Rowe et al., 2008; Morsy et al., 2021; Francey and Rowe, 2022; Samea and Abdelaal, 2023). However, for BGMs, exposing the edges of the coupons to the solution may directly affect the reinforcement layer and result in a fast degradation in the mechanical properties of BGM (Samea and Abdelaal, 2019). Thus, the edges of both BGMs were sealed with BGM strips, to ensure that the coupons were only exposed to the solution from the top bitumen coat and the back polymeric film.

The sealed BGM coupons (250 × 150 mm) and NW-GTX (190 × 100 mm) were immersed in a reduced synthetic MSW leachate. The chemistry of the leachate represents the different combinations of the primary constituents found in MSW landfill leachate collected from a landfill in Ontario, Canada (Hrapovic, 2001) including inorganic/organic salts, trace metals, and surfactant (Table 2). The leachate was reduced (Eh = -120 mV) to simulate anaerobic leachates found in MSW landfills. This

Table 2
Chemical composition of the synthetic Leachate (Abdelaal et al., 2014b) used in this study (mg/l except where noted).

Component	Formula	Concentration (mg/l, except where noted)
	Inorganic Salts	
Sodium Hydrogen Carbonate	$NaHCO_3$	3012
Calcium Chloride dihydrate	$CaCl_2{\cdot}2H_2O$	2882
Magnesium Chloride	$MgCl2{\cdot}6H_2O$	3114
Magnesium Sulphate heptahydrate	$MgSO_4{\cdot}7H_2O$	319
Ammonium Hydrogen Carbonate	NH_4HCO_3	2439
Carbamide (Urea)	$CO(NH_2)_2$	695
Sodium Nitrate	$NaNO_3$	50
Potassium Carbonate	K_2CO_3	324
Potassium Hydrogen Carbonate	$KHCO_3$	312
Potassium dihydrogen Phosphate	K_2HPO_4	30
	Trace Metals	
Ferrous Sulphate	$FeSO_4{\cdot}7H_2O$	2000
Boric Acid	H_3BO_3	50
Zinc Sulphate heptahydrate	$ZnSO_4{\cdot}7H_2O$	50
Cupric Sulphate, pentahydrate	$CuSO_4{\cdot}5H_2O$	40
Manganous Sulphate monohydrate	$MnSO_4{\cdot}H_2O$	500
Ammonium Molybdate tetrahydrate	$(NH_4)_6Mo_7O_{24}{\cdot}4H_2O$	50
Aluminum Sulphate, 16-hydrate	$Al_2(SO_4)_3{\cdot}16H_2O$	30
Cobaltous Sulphate, heptahydrate	$CoSO_4{\cdot}7H_2O$	150
Nickel (II) Sulphate	$NiSO_4{\cdot}6H_2O$	500
Sulfuric acid (+96% purity)	H_2SO_4 (ml/l)	1
	Other components	
Surfactant IGEPAL® CA720	$(C_2H_4O)n.C_{14}H_{22}O$, n ~ 12.5 (ml/l)	5
Eh (adjusted by adding 3% w/v $Na_2S{\cdot}9H_2O$) (mV)	$Na_2S{\cdot}9H_2O$ (ml/l)	0.94
Sulphuric acid for pH adjustment to pH ~ 7.0*	H_2SO_4 (ml/l)	0.7

* The pH was checked at the end of the 2-month refreshment cycles and was found to remain constant at ~ 7.

leachate was selected as it was extensively used in many GMB ageing studies (e.g., Abdelaal et al., 2014b; Rowe and Shoaib, 2017; Rowe et al., 2019; Francey and Rowe, 2022) and was shown to represent an aggressive simulation of MSW leachates. Hence it can allow the assessment of the relative performance of the two BGMs examined in a reasonable time.

The BGM coupons were placed in stainless steel containers filled with the leachate and incubated in forced-air ovens at different elevated temperatures (22, 40, 55 and 70 °C) while the NW-GTX coupons were only incubated at 55 °C. The solution was replaced every two months to maintain a constant pH for both BGMs and the NW-GTX. Specimens from the BGMs and NW-GTX were collected at different incubation times and examined using different index tests to assess their degradation.

2.3. Index testing

2.3.1. Rheology and chemical index tests

2.3.1.1. Dynamic shear rheometer. The effect of ageing at different temperatures on the rheological properties of the BGM was examined using an Anton Paar MCR102 Dynamic Shear Rheometer (DSR). This technique is widely used to characterize the viscous and elastic behaviour of bitumen in pavement research (e.g., Airey, 2003; Lu et al., 2008; Ragni et al., 2018; Omairey et al., 2020; Ding et al., 2022) and recently for BGMs in geoenvironmental applications (Samea and Abdelaal, 2023). Changes in rheological indices such as the complex shear modulus (G^*; representing the material resistance to shear deformation) and phase angle (δ; representing the balance in the elastic and viscous components of the bitumen) of the unaged and aged BGMs were measured in their linear viscoelastic region (LVE) using the linear amplitude sweep test. In this test, a constant normal force of 1 N was applied using a 25 mm parallel plate at a fixed frequency of 10 rad/s and under a strain level of 0.01% to 60% at a constant temperature of 55 °C. Ten specimens were examined in the DSR from each BGM, and despite the small difference in their unaged G^* and δ values (Table 1), the difference was statistically significant at the 95% confidence level. Although the two BGMs were manufactured from the same source bitumen, the small difference in their initial G^* and δ can be attributed to the difference in the thickness of the DSR samples from the two BGMs and its effect on the viscoelastic properties of the bitumen. For the aged samples, three replicates were examined at different incubation durations to assess the changes in G^* and δ with time relative to the unaged values.

2.3.1.2. Fourier transform infrared spectroscopy. Fourier Transform Infrared (FTIR) analysis was conducted to explore the changes in the functional groups of the polymer-modified bitumen due to oxidative degradation (Durrieu et al., 2007; Aguiar-Moya et al., 2017). For each data point, four specimens were prepared at 22 °C by extracting and dissolving the bitumen coat in toluene (10% bitumen by mass) and were then dried on a potassium bromide disk. Spectra in the wave number range of 4000 to 400 cm^{-1} obtained at a frequency of 32 and resolution of 4 cm^{-1} were analyzed using a Thermo Scientific Nicolet iS20 spectrometer to explore changes in the carbonyl (C═O) and butadiene double bond (C═C) functional groups at different incubation times. Changes in C═O can be used to infer the oxidation in the bitumen coat while the C═C reflects the degradation of the SBS copolymer (Mouillet et al., 2008; Zeng et al., 2015). The degree of ageing of the bitumen coat can be assessed using the carbonyl and butadiene indices (e.g., Lamontagne et al., 2001; de Sá Araujo et al., 2013; Feng et al., 2022) that can be calculated viz:

$$I_{C=O} = \frac{Area\ of\ the\ carbonyl\ band\ centered\ around\ 1700\ cm^{-1}}{\Sigma Area\ of\ the\ spectral\ bands\ between\ 4000\ and\ 600\ cm^{-1}} \quad (1)$$

$$I_{SBS} = \frac{Area\ of\ the\ carbonyl\ band\ centered\ around\ 968\ cm^{-1}}{\Sigma Area\ of\ the\ spectral\ bands\ between\ 4000\ and\ 600\ cm^{-1}} \quad (2)$$

Where; $I_{C=O}$ = carbonyl index, I_{SBS} = butadiene index.

The initial $I_{C=O}$ values of the unaged BGM1 and BGM2 (Table 1) were 0.00238 and 0.00199, respectively, while the initial I_{SBS} values were around 0.014 and 0.013, respectively. Since the samples extracted from the two BGMs and analyzed using the FTIR had similar thicknesses, the difference in the unaged $I_{C=O}$ and I_{SBS} of the two BGMs was statistically insignificant.

2.3.2. Mechanical index tests

Tensile properties of the BGMs and the NW-GTX were examined to assess the changes in mechanical strength (reported herein as the maximum/peak values) and the corresponding elongation due to ageing. Tensile tests on BGMs and the NW-GTX were conducted at the room temperature (22 °C) using a Zwick Roell universal testing machine (Model Z020). For the BGM, the initial separation between the machine grips was 60 mm and the samples were tested at a strain rate of 50 mm/min (ASTM D7275) while for the NW-GTX, an initial separation of 75 mm and a strain rate of 300 mm/min were used (ASTM D5035).

3. Results and discussion

3.1. Effect of the BGM thickness on the chemical and rheological properties

3.1.1. Complex shear modulus and phase angle

The initial G* values of the unaged BGM1 and BGM2 were 112 kPa and 134 kPa, respectively. For the initial δ, the values were 43° and 41° for BGM1 and BGM2 respectively, implying similar proportions of the viscous and elastic structures of the unaged BGMs (Hunter et al., 2015). After immersion in leachate, G^* gradually increased while δ decreased during the incubation period at 55 and 70 °C implying the increase of elastic components of the bitumen in both BGMs and the increase in the bitumen rigidity (Fig. 1a and 1b). The rates of change in G^* and δ for the two BGMs were faster at 70 °C than those at 55 °C. After 33 months of incubation at 70 °C, G^* gradually increased by a factor of 2.1 for BGM1 and 2.2 for BGM2. By the same time, δ decreased by 35% for BGM1 and by 40% for BGM2. Thus, the thinner BGM2 exhibited slightly more rheological changes than BGM1 and hence had more shift toward the elastic behaviour upon incubation at elevated temperatures.

3.1.2. Carbonyl and butadiene indices

The $I_{C=O}$ of both BGMs aged at elevated temperatures increased upon incubation in leachate and the rate of increase was higher at 70 °C than at 55 °C (Fig. 1c). This implies an increase in the oxidative degradation byproducts for both BGMs due to ageing at elevated temperatures. While the I_{SBS} data was highly scattered around the initial values, it decreased for both BGMs implying the degradation in the SBS-copolymer due to ageing in leachate that was also temperature dependent (Fig. 1d). After 33 months of incubation at 70 °C, $I_{C=O}$ increased by factors of 6 and 8.5 for BGM1 and BGM2, respectively, while the reduction in I_{SBS} was 17% for BGM1 and 20% for BGM2. Thus, the average oxidative degradation of the bitumen coat and the consumption of SBS-copolymer were slightly higher for the thinner BGM after incubation in leachate at elevated temperatures.

3.2. Effect of BGM thickness on the degradation in mechanical properties

The degradation in the tensile properties of the two BGMs was only observed at 70 and 55 °C (Fig. 2) while there was no change in these properties at 40 and 22 °C during the 33 months of incubation. Additionally, the two BGMs showed similar degradation behaviour in their tensile properties at different temperatures. For instance, the maximum tensile strength (σ_{max}) of BGM1 and BGM2 at 70 °C linearly decreased over 11 and 9 months, respectively, to reach 10% of the initial values, and stabilized at this value until 33 months (Fig. 2a). For the elongations at the maximum (peak) strength (ε_{max}), there was a gradual decrease to a stabilized value of 15% of the initial value that was reached after 9 months for BGM1 and 7 months for BGM2. Hence the degradation in ε_{max} was slightly faster than the degradation in σ_{max}. Since the degradation rates in the tensile properties were slightly faster for BGM2 than for BGM1, this suggests that the BGM thickness had a minor effect on the degradation of the two BGMs in leachate.

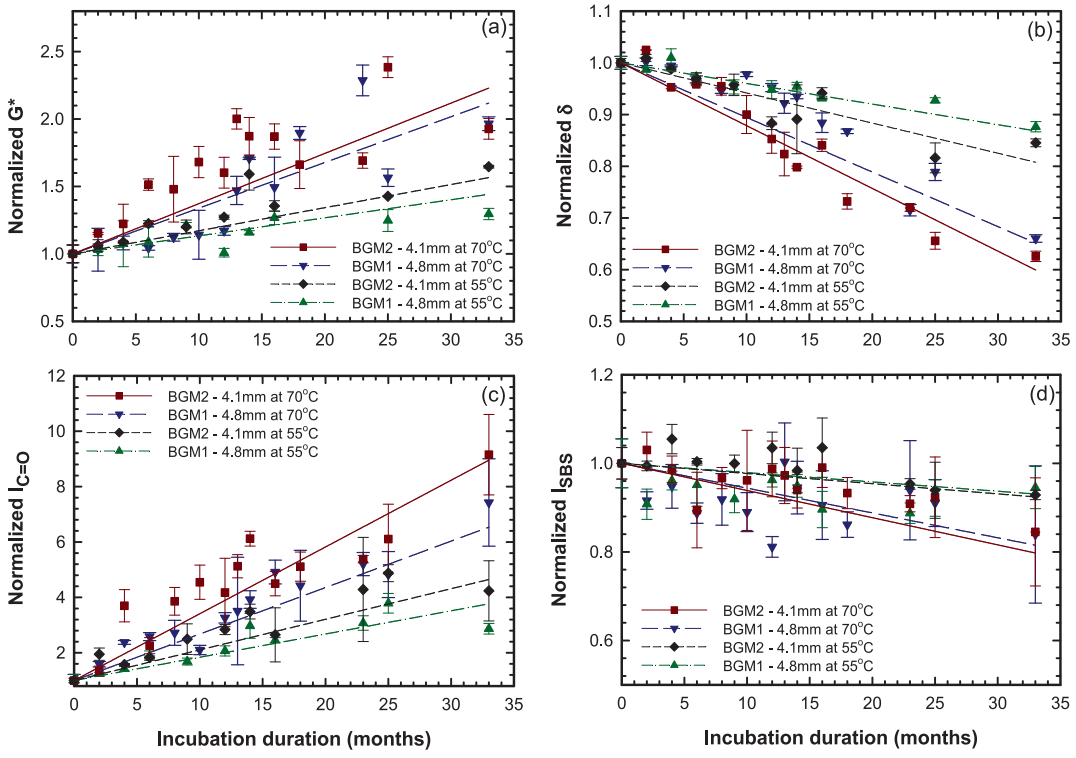

Fig. 1. Variation with incubation time for the BGM1 and the BGM2 in leachate at 70 and 55 °C in the normalized values (aged values/initial values) of the (a) complex shear modulus (G^*); (b) phase angle (δ); (c) carbonyl index ($I_{C=O}$); (d) butadiene index (I_{SBS}). (Note: unless otherwise noted, the data points presented in all the figures represent the mean value, while the error bars represent the ±1 standard deviation of the data).

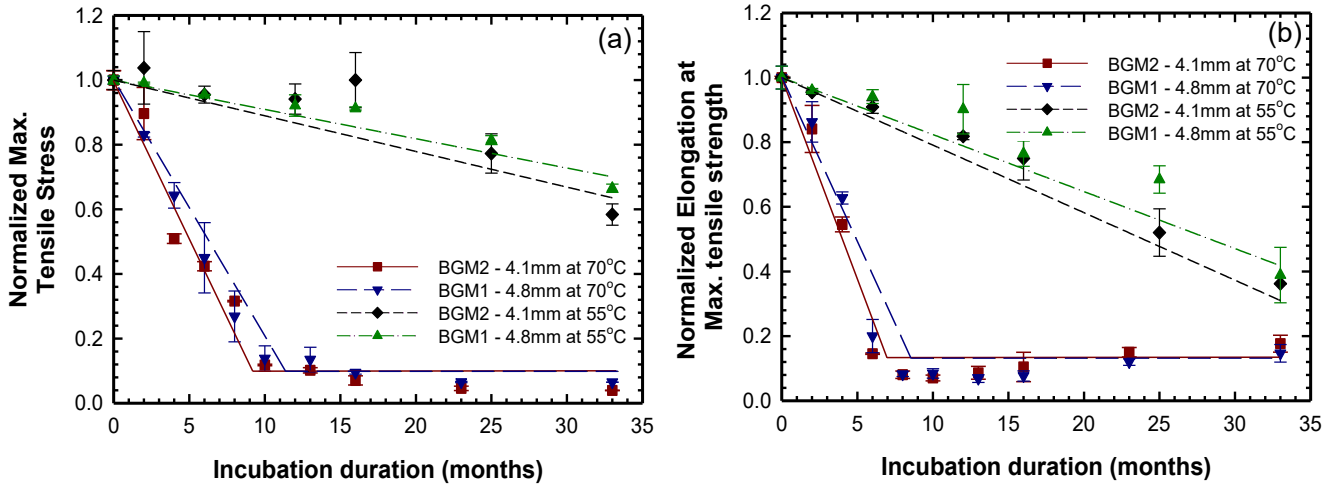

Fig. 2. Variation with incubation time for the BGM1 and the BGM2 in leachate at 70 and 55 °C in the normalized values (aged values/initial values) of the (a) machine direction tensile peak stress; (b) machine direction elongation at peak tensile stress.

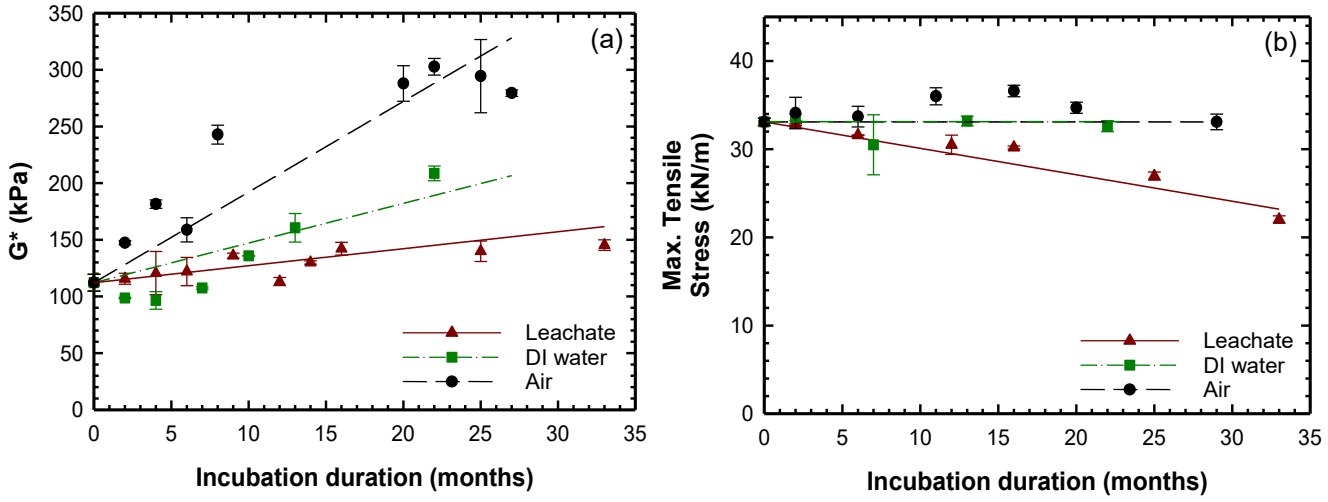

Fig. 3. Variation with incubation time for the BGM1 in different incubation media at 55 °C in the values of the (a) complex shear modulus; (b) machine direction tensile peak stress. Data in Air (humidity of 37%) and DI-Water are from Samea and Abdelaal (2023).

3.3. Discussion of the BGM degradation behaviour and thickness effect in MSW leachate

Incubation of BGM1 and BGM2 in leachate at elevated temperatures resulted in the thermo-oxidative degradation of the bitumen coat. This was inferred from the increase in C═O and the decrease in C═C functional groups. These changes led to an increase in bitumen stiffness evidenced by the increase in G^* and the decrease in δ. However, these changes in the bitumen coat in leachate were substantially lower than those measured for BGM1 in air (humidity of 37%) or DI water immersion (Samea and Abdelaal, 2023). For instance, after 25 months of incubation at 55 °C of BGM1, G^* was 2.1 and 1.3 times higher in air and DI water, respectively, than in leachate (Fig. 3a). Additionally, there was more scatter in data for the samples aged in air than in DI water and leachate implying that the severe oxidation across different parts of the samples exposed to air was non-uniform compared to the fully immersed samples in aqueous solutions. Likewise, incubation in air and DI water at 55 °C showed higher $I_{C=O}$ values by factors of 1.65 and 1.15 (Samea and Abdelaal, 2023), respectively, relative to leachate after 25 months. The observed slower oxidative degradation of the bitumen coat in leachate can be attributed to the reduced conditions of synthetic leachate and the absence of free oxygen relative to air or DI water ageing. Although exposure to the salts in the leachate is expected to accelerate the degradation of bitumen (Pang et al., 2018; Meng et al., 2022), the aforementioned results highlight that oxygen availability has more effect on the oxidative degradation of the bitumen coat.

While the changes in the bitumen coat were relatively low even at 70 °C for both BGMs in the MSW leachate, it seems that the bitumen coat was not protecting the reinforcement layers from degradation and the BGMs exhibited degradation in all mechanical properties. This fast degradation in the mechanical properties of the BGM in aqueous solutions can be attributed to the hydrolysis of the polyester fibres of the NW-GTX (Samea and Abdelaal, 2023) that was much faster in leachate than in DI water. For instance, for BGM1 at 55 °C in leachate, σ_{max} started to decrease just after incubation to reach 65% of the initial values after 33 months while in DI water, σ_{max} was retained at the initial values until 29 months (Fig. 3b). The faster degradation in leachate can be attributed to the presence of the surfactant that increases the BGM surface wettability and hence, potentially, the interaction of the H^+/OH^- ions and other chemical constituents of leachate with the NW-GTX than in DI water without the surfactant.

The hypothesized limited protection offered by the bitumen coat to the NW-GTX can be also inferred from comparing the degradation of BGM1 to the NW-GTX that was used in its formulation in leachate

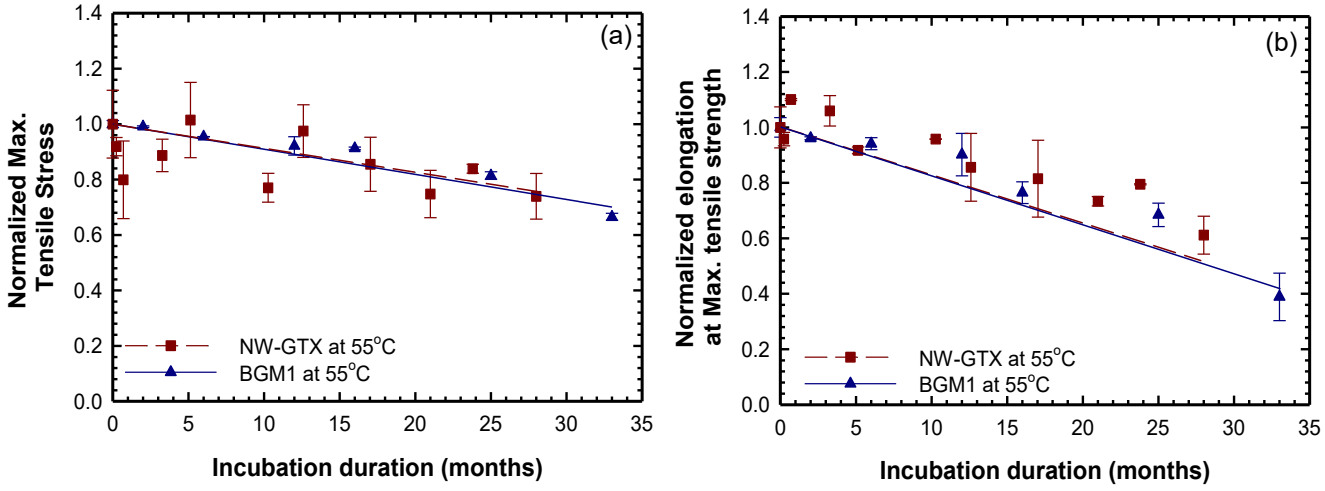

Fig. 4. Variation with incubation time for the BGM1 and the NW-GTX in MSW leachate at 55 °C in the normalized values (aged values/initial values) of the (a) machine direction tensile peak stress; (b) machine direction elongation at peak tensile stress.

(Fig. 4). After 33 months of incubation at 55 °C, the degradation in the tensile properties of the NW-GTX was similar to BGM1 with a slightly degraded bitumen coat. This also implies that in leachate, the chemical constituents of the solution can interact with the bitumen-impregnated and coated NW-GTX upon incubation at elevated temperatures. Another factor that may have contributed to such fast degradation of the NW-GTX was the degradation of the polymeric back film on the bottom surface of the BGM. In leachate at 70 °C, the film was completely detached and decomposed after only 6 months of immersion, while it remained intact for more than 20 months of immersion in both air and DI water. This resulted in the direct exposure of the bitumen coating the NW-GTX from both sides of the coupons and may have led to such faster degradation in the mechanical properties of the BGM.

The presence of the surfactant in leachate also seems to limit the effect of the BGM thickness on the degradation behaviour of BGM1 and BGM2. This is due to the ineffective increase in the resistance of the thicker bitumen coat to the migration of the chemical constituents of the leachate into the bitumen in the presence of the surfactant. Hence, increasing the BGM thickness from 4.1 to 4.8 mm showed an arguably slight decrease in the degradation of their bitumen coats and their NW-GTXs. Overall, the reduced conditions of leachate were favourable in terms of the degradation of the bitumen coat of the BGM relative to air and DI water immersion. However, the combination of the surfactant and the other chemical constituents of the leachate increased the degradation of the polymeric back film and the BGM reinforcement layer that resulted in faster degradation of mechanical properties in leachate than in air and DI water.

The degradation behaviour of BGMs at elevated temperatures discussed herein differs from the degradation of polymeric GMBs that starts with an antioxidant depletion stage then an induction period in which the properties are retained at the initial values, and finally the polymer degradation resulting in the loss of the different properties (e.g., Hsuan and Koerner, 1998). This is because, BGMs exhibit degradation in their properties upon incubation (e.g., Figs. 1 and 2) since they are not typically formulated with antioxidants. Additionally, the degradation of the multicomponent BGMs progresses simultaneously in the bitumen coat and the NW-GTX and the extent of the degradation in these different components depends on the incubation media as discussed above. Thus, unlike polymeric GMBs in which their degradation involves three sequential distinct stages, the BGM degradation initiates and propagates in one stage that simultaneously affects the bitumen coat and the NW-GTX. This required the holistic investigation of the chemical, rheological, and mechanical properties of the BGM to capture the degradation in these different components to assess its nominal failure (Samea and Abdelaal, 2023).

4. Arrhenius modelling and nominal failure predictions

Based on the criteria proposed by Samea and Abdelaal (2023),

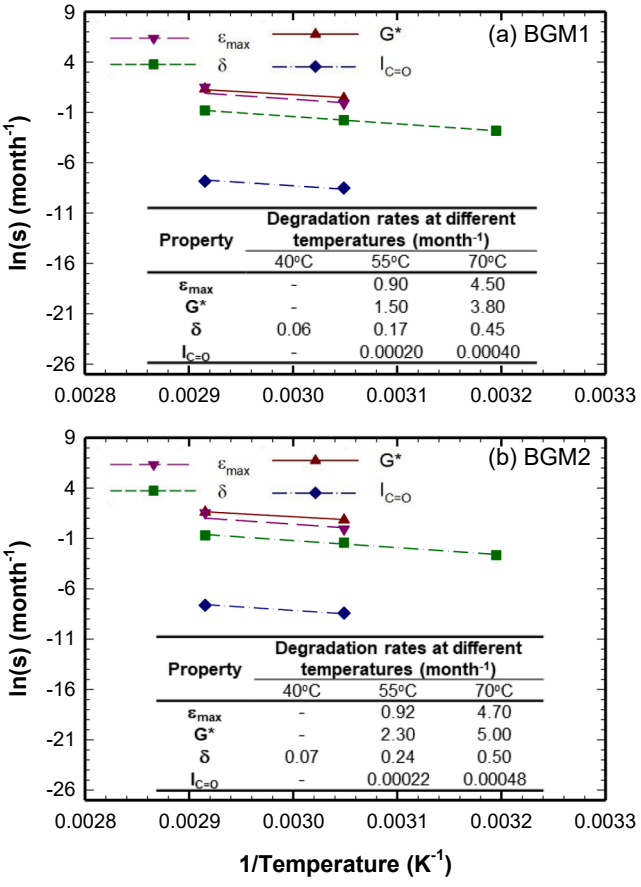

Fig. 5. Arrhenius plots and degradation rates of the elongation at peak tensile stress (ε_{max}), complex shear modulus (G^*), phase angle (δ), and carbonyl index ($I_{C=O}$) in leachate for: (a) BGM1; (b) BGM2. Degradation rates were not established for all properties at 22 °C during the 33-month incubation period.

nominal failure in the chemical and rheological properties of the BGM is reached at the time of brittleness of the bitumen coat when the measured values of G^*, δ and $I_{C=O}$ reach 640 kPa, 20° and 0.035, respectively. Similarly, time to nominal failure (t_{NF}) with respect to the mechanical properties can be estimated as the time at which ε_{max} reaches 50% of the minimum value specified by the manufacturer (Table 1). Because the degradation in all the BGM properties was initiated at 55 and 70 °C during the 33 months of incubation, the best-fit lines presented in Figs. 1 and 2 allowed the assessment of the degradation rates (i.e., the slopes) presented in Fig. 5. These degradation rates also allowed predicting the t_{NF} at these temperatures even if nominal failure was not reached during the 33 months of incubation, especially for the chemical and rheological properties since the bitumen coat did not reach brittleness even at 70 °C.

To estimate the degradation rates and hence the t_{NF} at temperatures that are not examined experimentally (i.e., lower field temperatures), time temperature superposition (Arrhenius modelling) is commonly used for polymeric and bituminous materials (e.g., Koerner et al., 1992; Rek and Barjaktarović, 2002; Rowe and Islam, 2009; Naskar et al., 2012; Rowe et al., 2019; Li et al., 2021). However, a single Arrhenius relation cannot be used to predict the overall degradation in the multicomponent BGMs due to the different reaction rates related to the different degradation mechanisms in their different components (Samea and Abdelaal, 2023). Alternatively, different Arrhenius plots (Fig. 5) were used to separately estimate the degradation rates in the mechanical properties (only related to the NW-GTX component) and in the chemical and rheological properties (only related to the bitumen coat) in leachate at lower field temperatures for the two BGMs viz:

$$s = A\, e^{-(Ea/RT)} \tag{3}$$

where, s (month^{-1}): degradation rate; A (month^{-1}): collision factor; E_a (J.mol^{-1}): activation energy; R (J.mol^{-1}.K^{-1}): universal gas constant equals 8.314; and T (K): temperature. Taking the natural logarithm of both sides of Eq. (3) gives:

$$ln(S) = ln(A) - (Ea/R) \times (1/T) \tag{4}$$

Despite the 33-month incubation duration, the t_{NF} predictions for BGM1 and BGM2 are preliminary since they were based only on two temperatures (except for δ with the degradation obtained at 3 temperatures). While predictions established based only on two elevated temperatures typically err on the conservative side (e.g., Ewais et al., 2018; Rowe et al., 2020), longer incubation time is required to establish the degradation rates at temperatures below 55 °C which will aid in refining the predictions at lower temperatures. However, to refine the predictions based on the available data, the t_{NF} predictions of ε_{max}, G^* and $I_{C=O}$ were also estimated using the activation energies reported by Samea and Abdelaal (2023) for BGM1 samples immersed in air and DI water, that were established based on 3-temperature Arrhenius plots. Table 3 shows the estimated t_{NF} of the two BGMs at typical landfill liner temperatures between 20 and 55 °C (i.e., below the lowest experimental temperatures at which degradation was obtained) based on the best fit E_a (using the degradation rates at 70 and 55 °C) and the E_a reported by Samea and Abdelaal (2023).

For the chemical and rheological properties, there was a small difference in the E_a values obtained from the slope of the Arrhenius plots for G^*, δ, and $I_{C=O}$ for BGM1 and BGM2 (Table 3 and Fig. 5). Since all these properties reflect the degradation of the bitumen coat, the difference in the E_a values may be related to the difference in the curve fitting to the data points of the different Arrhenius plots (i.e., degradation rates) established based only on two temperatures at the time of writing. Additionally, there was a slight variation in the E_a values obtained from Samea and Abdelaal (2023) based on the air and water immersion and the best-fit E_a from the leachate immersion reported herein. For example, for BGM1, the E_a values ranged between 48 and 64 kJ/mol for G^*, δ, and $I_{C=O}$, based on Samea and Abdelaal (2023) and from 43 to 60

Table 3
Predicted time to nominal failure (t_{NF}) in years of the two BGMs immersed in leachate (rounded to two significant digits).

Temperature (°C)	t_{NF} for BGM1 (Years)									
	Based on the activation energy from Samea and Abdelaal (2023)[a]				Based on the best fit activation energy[b]				Mean Predictions ± Standard deviation	
	ε_{max}	G*	δ	$I_{C=O}$	ε_{max}	G*	δ	$I_{C=O}$	Mechanical[c]	Brittleness[d]
20	40	225	175	180	260	370	150	90	150 ± 110	200 ± 85
30	18	115	74	83	66	170	67	50	42 ± 24	93 ± 40
40	8.4	63	33	41	19	80	31	29	14 ± 5	46 ± 19
50	4.2	36	15	21	5.6	40	15	17	4.9 ± 0.7	24 ± 10
55	3.0	27	11	15	3.2	29	11	14	3.1 ± 0.1	18 ± 7
E_a (kJ/mol)	59	48	64	56	100	58	60	43	–	–
Arrhenius equation	ln(s) = 21.6–7097/T	ln(s) = 18.8–5804/T	ln(s) = 21.6–7658/T	ln(s) = 12.1–6797/T	ln(s) = 36.7–12071/T	ln(s) = 21.6–6971/T	ln(s) = 20.2–7209/T	ln(s) = 7.3–5198/T	–	–
R^2	0.72	0.97	0.99	0.91	1	1	1	1	–	–
	t_{NF} for BGM2 (Years)									
20	31	145	144	160	235	160	110	105	130 ± 100	140 ± 22
30	14	75	60	74	59	84	50	55	37 ± 23	65 ± 12
40	6.6	41	27	36	16	45	23	30	11 ± 5	33 ± 8
50	3.3	23	13	18	4.8	25	12	16	4.1 ± 0.8	18 ± 5
55	2.3	17	8.8	13	2.7	19	8.3	12	2.5 ± 0.2	13 ± 4
E_a (kJ/mol)	59	48	64	56	101	48	59	48	–	–
Arrhenius equation	ln(s) = 21.7–7097/T	ln(s) = 18.6–5804/T	ln(s) = 21.8–7658/T	ln(s) = 12.2–6797/T	ln(s) = 37.2–12232/T	ln(s) = 18.53–5824/T	ln(s) = 19.9–7060/T	ln(s) = 9.4–5851/T	–	–
R^2	0.77	0.99	0.98	0.98	1	1	0.98	1	–	–

For ε_{max}, time to nominal failure was established based on the time to reach 50% of the minimum value specified by the manufacturer for these BGMs.
For G^*, δ, and $I_{C=O}$, time to nominal failure was established based on the time to brittleness of the bitumen coat when the values reach 620 kPa, 20°, and 0.035, respectively.

[a] Predictions estimated using the activation energies reported by Samea and Abdelaal (2023) for BGM1 samples immersed in air and DI water, established based on 3-temperature Arrhenius plots.

[b] Predictions based on the best fit activation energies using the degradation rates established experimentally at 70 and 55 °C in the current study.

[c] Average predictions using the activation energies from Samea and Abdelaal (2023) and the best fit activation energies based on ε_{max}.

[d] Average predictions using the activation energies from Samea and Abdelaal (2023) and the best fit activation energies based on time to brittleness (G^*, δ, and $I_{C=O}$).

kJ/mol based on the best fit from the current study. The similarity in the E_a values obtained from the different incubation media can be attributed to the similar mechanisms (i.e., thermo-oxidative degradation) governing the degradation of the bitumen coat in these different incubation media. For the Arrhenius plots of the mechanical properties that are related to the degradation of the NW-GTX, the E_a values obtained from the current study were twice the E_a values from Samea and Abdelaal (2023) for air immersion (Table 3). This big difference can be attributed to the difference in the degradation mechanism of the NW-GTX in air (thermal degradation) and the degradation of the NW-GTX by hydrolysis in aqueous solutions. To account for such variation in the E_a values given that they were established in the current study based only on two elevated temperatures, the average predictions of the t_{NF} established based on the E_a values from Samea and Abdelaal (2023) and those from the current study are also presented in Table 3.

In terms of the t_{NF}, the predictions at 55 °C based on ε_{max} ranged from 3 to 3.2 years for BGM1 and 2.3 to 2.7 years for BGM2 (Table 3). This was consistent with the current results, showing that the t_{NF} was not reached for BGM1 during the 33-month incubation period (~2.8 years), while it was experimentally observed after 2.7 years for BGM2. Likewise, the average predicted time to brittleness at 55 °C, was 18 and 13 years for BGM1 and BGM2 (Table 3), respectively, that exceeded the incubation period presented in the current study during which brittleness in the bitumen coat was not observed for both BGMs. This shows that range of the estimated t_{NF} based on the different E_a values in Table 3 was consistent with the experimentally observed degradation times at elevated temperatures for both BGMs during the 33-month incubation duration.

Among the different BGM properties, ε_{max} had the shortest t_{NF}, especially at elevated temperatures implying that the BGM may lose its mechanical properties before potentially losing its water tightness due to brittleness in the bitumen coat. For instance, at 30 °C, the estimated t_{NF} for BGM1 ranged between 18 and 66 years for ε_{max} and between 115 and 170 years for G^*, based on the two different activation energies used in establishing the predictions. The estimated t_{NF} for BGM2 based on ε_{max} at the same temperature ranged from 14 to 59 years. This shows that while the thicker BGM may seem slightly more durable at low field temperatures, the difference in predictions was statistically insignificant similar to the experimental data observed at elevated temperatures.

5. BGM performance in MSW synthetic leachate

Considering buried liners at the base of a waste disposal facility, the average predicted t_{NF} of the BGM liner based on the time brittleness in the bitumen coat (i.e., average predictions based on G^*, δ, and $I_{C=O}$) was greater than 100 years only for temperatures at or below 20 °C (Table 3). At a liner temperature of 40 °C which is typical for waste containment facilities that do not involve operations or wastes that generate elevated temperatures (Rowe and Islam, 2009, Rowe, 2012), the average predictions of the time to brittleness drop to 46 years for BGM1 and 33 years for BGM2. This shows the high sensitivity of the bitumen to temperature and its effect on the BGM durability. However, the predicted t_{NF} was substantially shorter when considering the degradation in the mechanical properties (14 years for BGM1 and 11 years for BGM2) due to the effect of the surfactant in leachate on the durability of the polyester NW-GTX. This implies that for containment applications that require long design lives, the examined BGMs may not be suitable for the containment of solid wastes containing surfactants since they result in fast degradation of their mechanical properties.

6. Conclusions

The effect of exposure to MSW leachate on the chemical, rheological and mechanical properties of two commercially available BGMs with nominal thicknesses of 4.8 and 4.1 mm was examined at four elevated temperatures (22, 40, 55 and 70 °C). Double-sided immersion tests were conducted using synthetic MSW leachate comprising a surfactant, trace metals, salts and a reducing agent. For the BGMs and testing conditions examined in this study, the following conclusions were reached:

1. The presence of surfactant in the MSW leachate increased the degradation of the polymeric back film and the reinforcement layer relative to incubation in DI water. This resulted in a faster degradation in the mechanical properties of the BGM than in the rheological and chemical properties of the bitumen coat.
2. The two BGMs exhibited slower degradation rates in the chemical and rheological properties of the bitumen coat in the MSW leachate than in DI water and air. This was attributed to the reduced conditions of the synthetic leachate examined.
3. While the 4.1 mm thick BGM had slightly faster degradation than the 4.8 mm thick BGM, the difference in the degradation rates of their bitumen coats and their NW-GTXs was insignificant at the elevated temperatures examined herein. This can be attributed to the ineffective increase in the resistance of the thicker bitumen coat to the migration of the chemical constituents of the leachate into the bitumen in the presence of the surfactant.
4. Predictions of the time to nominal failure of the BGMs at field temperatures between 20 and 55 °C showed high sensitivity of the BGM to the exposure temperatures. For example, the average estimated time to brittleness of the bitumen coat of BGM1 ranged from 200 ± 85 years at 20 °C to 18 ± 7 years at 55 °C. This highlights the need for considering the expected liner temperatures in the field when selecting BGMs for the barrier systems of waste containment applications.
5. Based on the predictions of nominal failure established using the different BGM properties, ε_{max} had the shortest t_{NF}, implying that the BGM may lose its mechanical properties before potentially losing its water tightness due to the brittleness of the bitumen coat.

The results presented in this study show the effect of thickness on the time to nominal failure for two elastomeric BGMs examined when immersed in synthetic leachate simulating landfill application. The results are relevant to the particular BGMs and conditions examined. The reported experiments involve double-sided exposure to leachate. Thus, the time to failure of the BGM in the field in which the BGM is exposed to the leachate from one side only is likely to be much longer than the predictions reported herein (Rowe et al., 2020). Further studies are also required to investigate the performance of BGMs in contact with landfill gases to examine their suitability for different solid waste containment applications.

Declaration of Competing Interest

The authors declare that they have no known competing financial interests or personal relationships that could have appeared to influence the work reported in this paper.

Data availability

Data will be made available on request.

Acknowledgement

The reported research in this paper was supported by the Natural Science and Engineering Research Council of Canada (NSERC) through the Discovery Grant program to F. B. Abdelaal (RGPIN-2018-04091). The equipment used was funded by the Canada Foundation for Innovation (CFI) and the Government of Ontario's Ministry of Research and Innovation. The authors acknowledge the contribution of Titan Environmental Containment Ltd. for providing the materials examined in this study.

References

Abdelaal, F.B., Rowe, R.K., 2014. Effect of high temperatures on antioxidant depletion from different HDPE geomembranes. Geotext. Geomembr. 42, 284–301. https://doi.org/10.1016/j.geotexmem.2014.05.002.

Abdelaal, F., Rowe, R., Brachman, R., 2014a. Brittle rupture of an aged HPDE geomembrane at local gravel indentations under simulated field conditions. Geosynthet. Int. 21 (1), 1–23. https://doi.org/10.1680/gein.13.00031.

Abdelaal, F.B., Rowe, R.K., Islam, M.Z., 2014b. Effect of leachate composition on the long-term performance of a HDPE geomembrane. Geotext. Geomembr. 42, 348–362. https://doi.org/10.1016/j.geotexmem.2014.06.001.

Addis, P., Andruchow, B. & Wislesky, I., 2013. Bituminous Geomembrane Failure at a Co-Disposal Tailings Storage Facility. Publisher: University of Alberta, Edmonton, Alberta, Canada. In: *17th International Conference on Tailings and Mine Waste*, 2013, Banff, AB, Canada, pp. 457-466. Doi: 10.7939/r3-ds53-4h45.

Alberta Environment Protection Agency, 2010. Standards for Landfills in Alberta. Alberta Environment Protection Agency. https://open.alberta.ca/dataset/b66da160-54f2-4c17-bd68-29d2aed1638b/resource/7c28c19d-e818-4495-abbc-03c62af29562/download/2010-standardslandfillsalberta-feb2010.pdf (Accessed 1 December 2022).

Aguiar-Moya, J.P., Salazar-Delgado, J., García, A., Baldi-Sevilla, A., Bonilla-Mora, V., Loría-Salazar, L.G., 2017. Effect of ageing on micromechanical properties of bitumen by means of atomic force microscopy. Road Mater. Pavement Des. 18, 203–215. https://doi.org/10.1080/14680629.2017.1304249.

Airey, G., 2003. Rheological properties of styrene butadiene styrene polymer modified road bitumens. Fuel 82, 1709–1719. https://doi.org/10.1016/S0016-2361(03)00146-7.

ASTM, 2013. Standard Test Method for Index Puncture Resistance of Geomembranes and Related Products. American Society for Testing and Materials D4833/D4833M, West Conshohocken, Pennsylvania, USA.

ASTM, 2015. Standard Test Methods for the Assignment of the Glass Transition Temperature by Modulated Temperature Differential Scanning Calorimetry. American Society for Testing and Materials E2602, West Conshohocken, Pennsylvania, USA.

ASTM, 2018. Standard Test Method for Measuring Mass per Unit Area of Geotextiles". American Society for Testing and Materials D5261, West Conshohocken, Pennsylvania, USA.

ASTM, 2018. Standard Test Method for Tensile Properties of Bituminous Geomembranes (BGM). American Society for Testing and Materials D7275, West Conshohocken, Pennsylvania, USA.

ASTM, 2019. Standard Test Method for Breaking Force and Elongation of Textile Fabrics (Strip Method). American Society for Testing and Materials D5035, West Conshohocken, Pennsylvania, USA.

ASTM, 2019. Standard Test Method for Measuring the Nominal Thickness of Geosynthetics". American Society for Testing and Materials D5199, West Conshohocken, Pennsylvania, USA.

Bannour, H., Barral, C., Touze-Foltz, N., 2013. Flow rate in composite liners including GCLs and a bituminous geomembrane. In: Proceedings of the 3rd International Conference on Geotechnical Engineering, 2013, In W. Frikha (Ed.), Hamamet, Tunisia, Vol. S5–9, pp. 809–819.

Breul, B., Reinson, J., Eldridge, T., G, S., Harmon, A., 2006. Bituminous Geomembrane in Extremely Cold Conditions. In: Proceedings of the International Conference of Geosynthetics, Rotterdam, Netherlands, pp. 395-398.

Breul, B., Huru, M., Palolahti, A., 2008. Use of bituminous geomembrane (BGM) liner for agnico eagle mine in Kittila (Finland). In: 4th European Geosynthetics Conference, 2008, Scotland. Paper number 245.

British Columbia Ministry of Environment, 2016. Landfill Criteria for Municipal Solid Waste, 2nd ed. British Columbia Ministry of Environment, British Columbia, p. 76. Accessed 1 December 2022.

Daly, N., Breul, B., 2017. Exceptional Longevity of Bituminous Geomembrane Through Several Decades of Practice. In: Proceedings of 70th Canadian Geotechnical Conference, 2017, Ottawa, Canada. Publisher: Canadian Geotechnical Society, Surrey, BC, Canada.

De Sá Araujo, M.D.F.A., Lins, V.D.F.C., Pasa, V.M.D., Leite, L.F.M., 2013. Weathering aging of modified asphalt binders. Fuel Process. Technol. 115, 19–25. https://doi.org/10.1016/j.fuproc.2013.03.029.

Ding, Y., Li, D., Zhang, H., Deng, M., Mao, X., Cao, X., 2022. Investigation of Aging Behavior of Asphalt under Multiple Environmental Conditions. J. Mater. Civ. Eng. 34, 04021419. https://doi.org/10.1061/(ASCE)MT.1943-5533.0004048.

Durrieu, F., Farcas, F., Mouillet, V., 2007. The influence of UV aging of a Styrene/Butadiene/Styrene modified bitumen: Comparison between laboratory and on site aging. Fuel 86, 1446–1451. https://doi.org/10.1016/j.fuel.2006.11.024.

Ewais, A., Rowe, R.K., Rimal, S., Sangam, H.P., 2018. 17-year elevated temperature study of HDPE geomembrane longevity in air, water and leachate. Geosynthet. Int. 25, 525–544. https://doi.org/10.1680/jgein.18.00016.

Ewais, A.M.R., Rowe, R.K., Scheirs, J., 2014. Degradation behaviour of HDPE geomembranes with high and low initial high-pressure oxidative induction time. Geotextiles and Geomembranes 42 (2), 111–126. https://doi.org/10.1016/j.geotexmem.2014.01.004.

Feng, B., Wang, H., Li, S., Ji, K., Li, L., Xiong, R., 2022. The durability of asphalt mixture with the action of salt erosion: A review. Constr. Build. Mater. 315, 125749 https://doi.org/10.1016/j.conbuildmat.2021.125749.

Francey, W., Rowe, R.K., 2022. Long-term Stress Crack Resistance of HDPE Fusion Seams Aged at 85° C in Synthetic Leachate. Can. Geotech. J. https://doi.org/10.1139/cgj-2022-0159.

Gassner, F., 2017. Development and management of geomembrane liner hippos. Geotext. Geomembr. 45 (6), 702–706. https://doi.org/10.1016/j.geotexmem.2017.08.007.

Hoor, A., Rowe, R.K., 2012. Application of tire chips to reduce the temperature of secondary geomembranes in municipal solid waste landfills. Waste Manag. 32, 901–911. https://doi-org.proxy.queensu.ca/10.1016/j.wasman.2011.12.026.

Hrapovic, L., 2001. Laboratory Study of Intrinsic Degradation of Organic Pollutants in Compacted Clayey Soil. The University of Western Ontario. PhD Thesis.

Hsuan, Y., Koerner, R., 1998. Antioxidant depletion lifetime in high density polyethylene geomembranes. J. Geotech. Geoenviron. Eng. 124, 532–541. https://doi.org/10.1061/(ASCE)1090-0241(1998)124:6(532).

Hunter, R. N., Self, A., Read, J., 2015. The shell bitumen handbook, ICE Publishing, London, UK. Doi: 10.1680/tsbh.58378.

Keys, H., 2021. Townsville undertakes Australia first geomembrane landfill rehabilitation [Online]. Waste Management Review. Available: https://wastemanagementreview.com.au/townsville-undertakes-australia-first-geomembrane-landfill-rehabilitation/ (Accessed 1 December 2022).

Koerner, R.M., Lord, A.E., Hsuan, Y.H., 1992. Arrhenius modeling to predict geosynthetic degradation. Geotext. Geomembr. 11, 151–183. https://doi.org/10.1016/0266-1144(92)90042-9.

Lamontagne, J., Dumas, P., Mouillet, V., Kister, J., 2001. Comparison by Fourier transform infrared (FTIR) spectroscopy of different ageing techniques: application to road bitumens. Fuel 80, 483–488. https://doi.org/10.1016/S0016-2361(00)00121-6.

Lazaro, J., Breul, B., 2014. Bituminous geomembrane in heap leach pads. In: Proceedings of Heap Leach Solutions, Lima, Peru, pp. 291-303. InfoMine Inc., Canada.

Li, W., Xu, Y., Huang, Q., Liu, Y., Liu, J., 2021. Antioxidant depletion patterns of high-density polyethylene geomembranes in landfills under different exposure conditions. Waste Manag. 121, 365–372. https://doi.org/10.1016/j.wasman.2020.12.025.

Lu, X., Talon, Y., Redelius, P., 2008. Ageing of bituminous binders - laboratory tests and field data. In: Proceedings of the 4th Eurasphalt & Eurobitume Congress, European Asphalt Pavement Association (EAPA), Copenhagen. Denmark, pp. 21-23.

Maisonneuve, C., Pierson, P., Duquennoi, C., Morin, A., 1997. Accelerated aging tests for geomembranes used in landfills. In: Proceedings of the 6th International Landfill Symposium, Cagliari, Sardinia, Italy. pp. 207–216.

Meng, Y., Hu, C., Tang, Y., Großegger, D., Qin, W., 2022. Investigation on the erosion mechanism of simulated salt conditions on bitumen. Constr. Build. Mater. 334, 127267 https://doi.org/10.1016/j.conbuildmat.2022.127267.

MOE, 1998. Landfill Standards. Landfill standards: A Guideline on the regulatory and approval requirements for new or expanding landfilling sites. Ontario Ministry of the Environment. Queen's Printer for Ontario, Toronto.

Morsy, M.S., Rowe, R.K., Abdelaal, F.B., 2021. Longevity of 12 geomembranes in chlorinated water. Can. Geotech. J. 58 (4), 479–495. https://doi.org/10.1139/cgj-2019-0520.

Mouillet, V., Farcas, F., Besson, S., 2008. Ageing by UV radiation of an elastomer modified bitumen. Fuel 87 (12), 2408–2419. https://doi.org/10.1016/j.fuel.2008.02.008.

MPCA, 2005. Demolition Landfill Guidance. Minnesota Pollution Control Agency. Water/Solid Waste #5.04, pp. 1–13. Available at: www.co.lake.mn.us/document_center/w_sw5_04.pdf (Accessed 1 December 2022).

Naskar, M., Reddy, K.S., Chaki, T.K., Divya, M.K., Deshpande, A.P., 2012. Effect of ageing on different modified bituminous binders: comparison between RTFOT and radiation ageing. Mater. struct. 46 (7), 1227–1241. https://doi.org/10.1617/s11527-012-9966-3.

Omairey, E.L., Zhang, Y., Gu, F., Ma, T., Hu, P., Luo, R., 2020. Rheological and fatigue characterisation of bitumen modified by anti-ageing compounds. Constr. Build. Mater. 265, 120307 https://doi.org/10.1016/j.conbuildmat.2020.120307.

Pang, L., Zhang, X., Wu, S., Ye, Y., Li, Y., 2018. Influence of Water Solute Exposure on the Chemical Evolution and Rheological Properties of Asphalt. Mater. (Basel). 11, 983. https://doi.org/10.3390/ma11060983.

Peggs, I., 2008. Prefabricated bituminous geomembrane: a candidate for exposed geomembrane caps for landfill closures. In: Proceedings of the first Pan American Geosynthetics Conference and Exhibition, Cancun, Mexico, Industrial Fabrics Association International (IFAI), USA, pp. 191-197.

Ragni, D., Ferrotti, G., Lu, X., Canestrari, F., 2018. Effect of temperature and chemical additives on the short-term ageing of polymer modified bitumen for WMA. Mater. Des. 160, 514–526. https://doi.org/10.1016/j.matdes.2018.09.042.

Rek, V., Barjaktarović, Z.M., 2002. Dynamic mechanical behavior of polymer modified bitumen. Mater. Res. Innovations. 6 (2), 39–43. https://doi.org/10.1007/s10019-002-0159-5.

Richardson, D., Wingrove, P., 2021. SRWRA Western Side Liner, Adelaide [PowerPoint slides]. https://www.wmrr.asn.au/common/Uploaded%20files/ALTS/2021/Don%20Richardson.pdf. (Accessed 1 December 2022).

Rowe, R.K., 2012. Short and long-term leakage through composite liners. The 7th Arthur Casagrande Lecture. Can. Geotech. J. 49 (2), 141–169. https://doi.org/10.1139/t11-092.

Rowe, R.K., Ewais, A.M.R., 2014. Antioxidant depletion from five geomembranes of same resin but of different thicknesses immersed in leachate. Geotext. Geomembr. 42, 540–554. https://doi.org/10.1016/j.geotexmem.2014.08.001.

Rowe, R.K., Abdelaal, F.B., Zafari, M., Morsy, M.S., Priyanto, D.G., 2020. An approach to high-density polyethylene (HDPE) geomembrane selection for challenging design requirements. Canadian Geotechnical Journal 57 (10), 1550–1565. https://doi.org/10.1139/cgj-2019-0572.

Rowe, R.K., Caers, C.J., Reynolds, G., Chan, C., 2000. Design and construction of the barrier system for the Halton Landfill. Can. Geotech. J. 37, 662–675. https://doi.org/10.1139/t99-131.

Rowe, R.K., Abdelaal, F.B., Islam, M.Z., 2014. Aging of High-Density Polyethylene Geomembranes of Three Different Thicknesses. J. Geotech. Geoenviron. Eng. 140 https://doi.org/10.1061/(asce)gt.1943-5606.0001090.

Rowe, R., Islam, M., Hsuan, Y., 2008. Leachate chemical composition effects on OIT depletion in an HDPE geomembrane. Geosynthet. Int. 15, 136–151. https://doi.org/10.1680/gein.2008.15.2.136.

Rowe, R.K., Islam, M.Z., 2009. Impact of landfill liner time–temperature history on the service life of HDPE geomembranes. Waste Manag. 29, 2689–2699. https://doi-org.proxy.queensu.ca/10.1016/j.wasman.2009.05.010.

Rowe, R.K., Morsy, M., Ewais, A., 2019. Representative stress crack resistance of polyolefin geomembranes used in waste management. Waste Manag. 100, 18–27. https://doi.org/10.1016/j.wasman.2019.08.028.

Rowe, R.K., Sangam, H.P., 2002. Durability of HDPE geomembranes. Geotext. Geomembr. 20, 77–95. https://doi.org/10.1016/S0266-1144(02)00005-5.

Rowe, R.K., Shoaib, M., 2017. Long-term performance of high-density polyethylene (HDPE) geomembrane seams in municipal solid waste (MSW) leachate. Can. Geotech. J. 54, 1623–1636. https://doi.org/10.1139/cgj-2017-0049.

Rowe, R.K., Sangam, H.P., Lake, C.B., 2003. Evaluation of an HDPE geomembrane after 14 years as a leachate lagoon liner. Can. Geotech. J. 40, 536–550. https://doi.org/10.1139/t03-019.

Rowe, R.K., Quigley, R.M., Brachman, R.W., Booker, J.R., 2004. Barrier systems for waste disposal facilities. Taylor & Francis Books Ltd. (E & FN Spon), London.

Rowe, R.K., Islam, M.Z., Hsuan, Y.G., 2010. Effects of Thickness on the Aging of HDPE Geomembranes. J. Geotech. Geoenviron. Eng. 136, 299–309. https://doi.org/10.1061/(asce)gt.1943-5606.0000207.

Samea, A., Abdelaal, F.B., 2023. Effect of elevated temperatures on the degradation behaviour of elastomeric bituminous geomembranes. Geotext. Geomembr. 51 (1), 219–232. https://doi.org/10.1016/j.geotexmem.2022.10.010.

Samea, A., Abdelaal, F.B., 2019. Chemical durability of bituminous geomembranes in heap leaching applications at 55oC. In: Proceedings of Geosynthetics 2019 Conference, Houston, Texas, USA, pp. 298-308. Industrial Fabrics Association International (IFAI), USA.

Scheirs, J., 2009. A guide to polymeric geomembranes: a practical approach. John Wiley & Sons, West Sussex, United Kingdom.

Schmidt, R., Young, C., Helwitt, J., 1984. Long term field performance of geomembranes fifteen years experience. The International Conference on Geomembranes 1984, 173–187.

Tian, K., Benson, C.H., Tinjum, J.M., Edil, T.B., 2017. Antioxidant depletion and service life prediction for HDPE geomembranes exposed to low-level radioactive waste leachate. J. Geotech. Geoenviron. Eng. 143 (6), 1–11. https://doi.org/10.1061/(ASCE)GT.1943-5606.0001643.

Touze-Foltz, N., Farcas, F., 2017. Long-term performance and binder chemical structure evolution of elastomeric bituminous geomembranes. Geotext. Geomembr. 45, 121–130. https://doi.org/10.1016/j.geotexmem.2017.01.003.

USEPA, U.S. Environmental Protection Agency, 2016. Advancing sustainable materials management: 2014 fact sheet. USEPA, Washington, DC.

Zeng, W., Wu, S., Wen, J., Chen, Z., 2015. The temperature effects in aging index of asphalt during UV aging process. Constr. Build. Mater. 93, 1125–1131. https://doi.org/10.1016/j.conbuildmat.2015.05.022.